Some Aspects of Overturning Mechanisms of Pile Driving Machine on Soft Foundation

Shouji Toma[1, *], Wai Fah Chen[2]

[1](Formerly) Department of Civil Engineering, Hokkai-Gakuen University, Sapporo, Japan

[2](Formerly) Department of Civil Engineering, University of Hawaii, Manoa, USA

Email address:

toma@hgu.jp (Shouji Toma), chenwilfred@gamil.com (Wai Fah Chen)

[*]Corresponding author

To cite this article:

Abstract: Many overturning accidents of cranes and pile driving machines have occurred in recent years. Overturning mechanisms of those accidents have been studied by the author, et al., based on theory of structural stability by using the rotational spring-rigid bar model. A summary of the theoretical study is first described in this paper including the concept of the structural stability, the category of the overturning mechanisms and the preliminary model test. Then, using the same structural model, the computer structural analysis, in which software TDAPIII (Time-domain Dynamic Analysis Program in 3-dimension) is used, is explained in order to compare with the previous theoretical study. Consequently, the computer analysis confirms a good coincidence with the theoretical results. Further, by the computer analysis, the effect of the rotational stiffness of the foundation and the eigenvalue analysis to find the critical load are studied. In general, the computer analysis is a more practical tool to study the overturning mechanism than the theoretical analysis which is based on the equilibrium equations. The computer analysis would be possible to consider the material non-linearity of the foundation and 3-dimensional effect. In order to avoid this kind of overturning accident in the future, the results in this paper will give useful information to study further in details.

Keywords: Overturning Mechanism, Pile Driving Machine, Crane, Structural Stability, Soft Foundation, Computer Structural Analysis, Effect of Initial Imperfections

1. Introduction

Recently, overturning accidents of pile driving machines and cranes have been often occurred [1, 2]. Figure 1 shows a typical accident in Japan. Once this kind of accident occurred the damage would be serious because the machines are so large and heavy. There are no official guidelines in the United States for the design and construction of safe working platforms for the machines, and so there is no official procedure to mitigate these potentially catastrophic risks [2]. The Pile Driving Contractors Association (PDCA) in the United States has a great concern on this issue and continues studying how to provide the safe working platforms at the construction site [3, 4].

The overturning mechanisms on soft foundation have been studied theoretically by the author et al. to find the cause based on the structural stability theory [5, 6]. In those previous studies the overturning mechanisms are categorized into the following three:

(1) Type of overturning moment;

(2) Type of structural instability;

(3) Type of equilibrium transition.

Firstly, (1) Type of overturning moment is a case that the displacement angle exceeds the stability limit angle at which the overturning moment exceeds the resisting moment. Secondly, (2) Type of structural instability is a case that the vertical load exceeds the critical load like the buckling of elastic columns. Lastly, (3) Type of equilibrium transition is a case that the displacement exceeds the limit angle when the machine is moving to the equilibrium position. These

mechanisms will be summarized in this paper. The theoretical results are confirmed by the computer analysis which is generally a more practical tool than the theoretical analysis for the overturning problem on the soft foundation [7].

Not only the overturning moment but also the instability could be a cause of an accidental collapse of the structures. Since the instability makes the structures deform in different direction from the load, it is difficult to predict the collapse without understanding the nature of instability. There were many accidental collapses due to the instability such as scaffolding failure, bridge girder fall, etc., in Japan [1, 8, 9]. The overturning of the pile driving machine may be considered one of them.

Since this paper basically follows the theory of structural stability, its concept with regard to the pile driving machine is first discussed in the next section.

Figure 1. *Overturning accident (04/19/2014) (with courtesy of Sankei Shimbun).*

2. Concept of Stability and Instability

Figure 2 shows the stability category of the pile driving machines displacement-wise, which is based on the mechanism (1) Type of overturning moment: (a) stable, (b) neutral and (c) unstable. In (a) stable region, the overturning moment is less than the resisting moment $Mt<Mr$; at (b) neutral, Mt is equal to Mr; and in (c) unstable region, $Mt>Mr$. This is a common classification and process to investigate the cause of the overturning accidents [10].

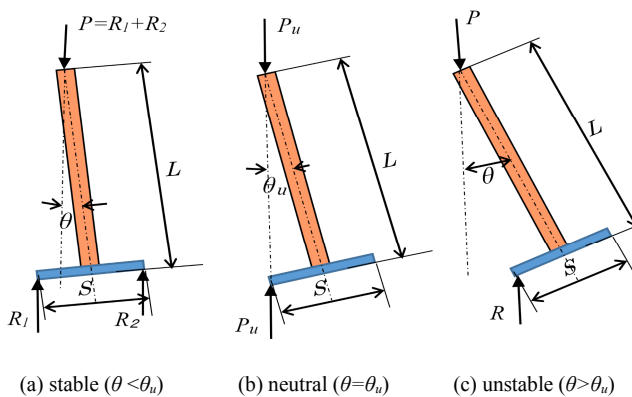(a) stable ($\theta<\theta_u$)   (b) neutral ($\theta=\theta_u$)   (c) unstable ($\theta>\theta_u$)

Figure 2. *Category of stability, deformation-wise.*

However, the overturning of pile driving machine on the "soft foundation" has to be discussed in view of the structural stability. Figure 3 is the stability surface which explains schematically the stability category load-wise based on the mechanism (2) Type of structural instability [11]. Here, the stability status of the structures can be expressed by the same three status as before: (a) stable, (b) neutral and (c) unstable, but in different way, i.e., load-wise. In the stable region of Figure 3, the ball (displacement) will return to the equilibrium position (center); in the unstable region, the ball will drop and the displacement will never return; and the boundary of the two is the neutral which is the eigenvalue load to overturn like the Euler buckling load in elastic columns.

Figure 4 is the stability curve which shows a certain section of Figure 3 at a load P in the stable region [5]. Since the load is in the stable region at B' load-wise, the ball (displacement) will tend to return to the equilibrium position at the center C'. If between B' and C' there is the stability limit which is defined by the mechanism (1) Type of overturning, the machine will move into the unstable region displacement-wise in Figure 2 (c). In this case, although the machine is still in the stable region load-wise, it is in the unstable region in displacement-wise, thus the machine will overturn. This is the overturning mechanism (3) Type of equilibrium transition and is considered what happened in the overturning accidents on the "soft foundation". This mechanism is a main theme of this paper.
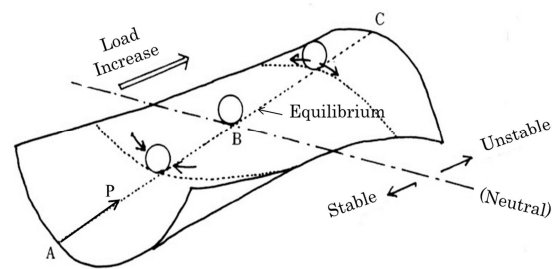

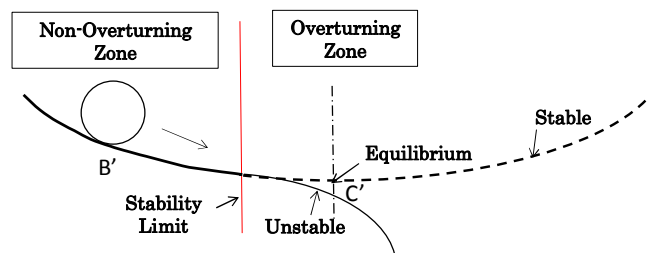**Figure 3.** *Stability surface, load-wise.*

Figure 4. *Stability curve.*

3. Structural Stability Analysis

3.1. Equilibrium Equations

The equilibrium equations, when the pile driving machine is on the soft foundation, are derived previously including the initial imperfections such as the initial inclination and the eccentricity of the load [5, 6]. A brief description will be given in this section. The structural model for the analysis is the

rigid bar-rotational spring system as shown in Figure 5, in which the left and right figures are before and after deformation, respectively. The equilibrium relation between the righting moment and the overturning moment in the right figure of Figure 5 leads to Eq. (1).

$$Ks(\theta - \theta o) - P(L\sin\theta + e\cos\theta) = 0 \qquad (1)$$

in which P=machine weight (=vertical support force at ground), L=load height, Ks=stiffness of rotational spring, θ=displacement angle, θo=initial inclination, and e=eccentric distance to load.

It should be noticed that the righting moment of the first term in Eq. (1) is assumed to increase linearly as the displacement increases. Therefore, Eq. (1) is only valid in the stable region in Figures 2 and 3, or in the non-overturning zone in Figure 4.

Transforming Eq. (1) for the load P gives

$$P = \frac{Ks(\theta - \theta o)}{L\sin\theta + e\cos\theta} \qquad (2)$$

Assuming the initial imperfections θ_o =0 and e=0, and the displacement θ is infinitesimally small, Eq. (2) becomes the eigenvalue as Eq. (3) [5, 6].

$$Pcr = Ks / L \qquad (3)$$

The critical load Eq. (3) corresponds to the Euler elastic buckling load of columns. Non-dimensionalizing Eq. (2) by Eq. (3) gives

$$\frac{P}{Pcr} = \frac{\theta - \theta o}{\sin\theta + e\cos\theta / L} \qquad (4)$$

On the other hand, the stability limit θu can be obtained based on the mechanism (1) Type of overturning moment by equating the resisting moment and the overturning moment in Figure 2 (b) as follows [10]:

$$\theta u = \tan^{-1} S / (2L) \qquad (5)$$

This stability limit angle is the boundary between the stable and unstable displacement-wise.
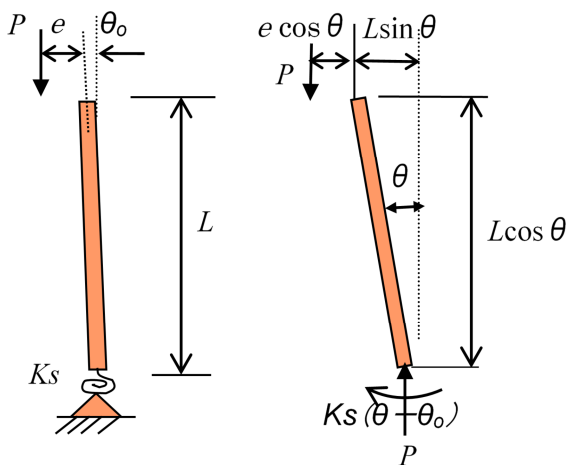

Figure 5. Structural Model.

3.2. Effect of Initial Inclination

The pile driving machine has a relative high center of gravity comparing to other heavy machines. Therefore, the initial imperfections such as the initial inclination and the eccentricity of the load affects significantly to enhance overturning. The equilibrium equations in the previous section include the initial imperfections. Here, by assuming the initial inclination θo exists but no eccentricity e=0 in Eq. (4), the equilibrium curves are plotted in Figure 6 for different initial inclinations [5, 6]. The vertical line of the stability limit angle is shown just for explanation purpose for the time being, which should be obtained by Eq. (5).

It can be seen from Figure 6 that the initial inclination lowers significantly the load-displacement curves. The intersections of the equilibrium curves and the stability limit indicate the overturning strength of the machine. For example, when the initial inclination θo is 0.1radian, the overturning strength is reduced almost by half of the critical load Pcr. If the displacement θ is small enough, i.e., $\sin\theta \approx \theta$ is valid, Eq. (4) will be Pu/Pcr=1-θo /θu, in which Pu is the overturning load and θu is the corresponding overturning displacement angle (stability limit). This relation is shown in Figure 7, which expresses the initial inclination lowers the overturning load linearly by the ratio θo /θu.
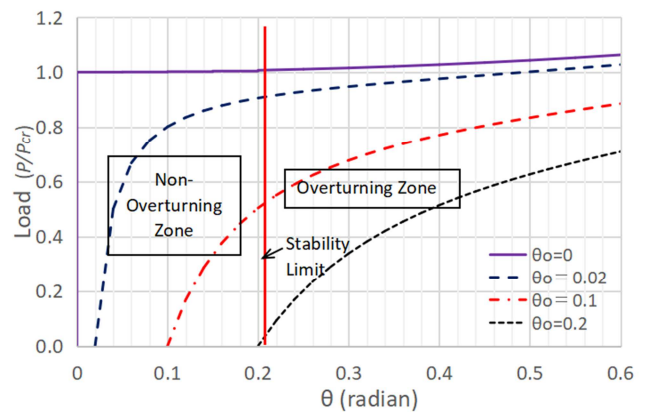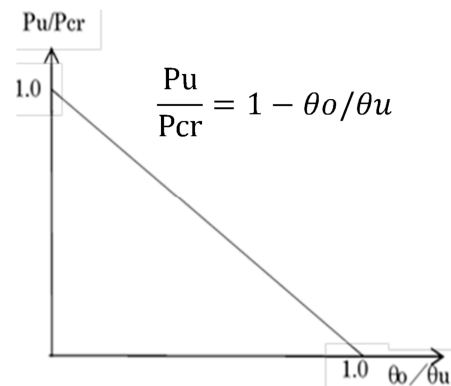

Figure 6. Effect of initial inclination.

Figure 7. Reduction rate by initial inclination.

3.3. Equilibrium in Unstable Region

As stated above, the equilibrium equations of Eqs. (1)

through (4) are only valid in the stable region. The equilibrium path beyond the stability limit will be discussed in this section. The equilibrium equation in the unstable region can be derived from Figure 2 (c) as follows:

$$R \, (S/2)\cos\theta - PL\sin\theta = 0 \qquad (6)$$

Figure 8 is a typical load-displacement curve taken from Figure 6. The reaction force R in Eq. (6) should not be more than the foundation strength Pu which is given by the intersection of the stability limit and the load-displacement curves. Substituting Pu for R in Eq. (6), the equilibrium path in the unstable region is obtained as shown in Figure 8, i.e., a descendent curve. There, it can be seen that the load will decrease as the displacement increases, namely unstable.
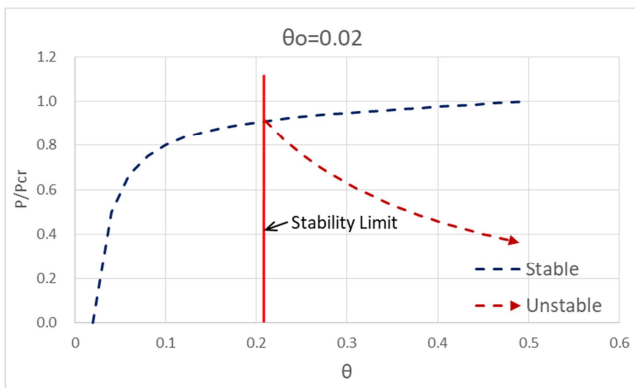

Figure 8. Equilibrium in unstable region.

4. Overturning Mechanism on Soft Foundation

4.1. Displacement Path on P-θ Curves

In this section, the overturning mechanism (3) Type of equilibrium transition will be described using the load-displacement curves [5, 6]. For example, let us look at Figure 9 which is the load-displacement curves calculated by Eq. (4) with the eccentricity e/L=0.185. Suppose the machine is at the equilibrium positon A presently, then the operator moves it to the position B' on the soft foundation. There, since the overturning moment becomes larger than the righting moment in Eq. (1), the machine is supposed to move to the right, the point C', in order to maintain the equilibrium. This means that as soon as the operator moves the machine to the soft ground unknowingly, the machine will start to incline slowly until reaches to the equilibrium.

If on the half way this transitional path from B' to C' crosses the stability limit, the machine will overturn. In another words, if the equilibrium position C' is at the left side of the stability limit (the stable zone), the machine will stay at C'. However, if the equilibrium position C' is at the right side of the stability limit (the overturning zone), the machine will be overturning, presumably faster after passing the stability limit. This type of mechanism was also described by the stability curve in Figure 4.
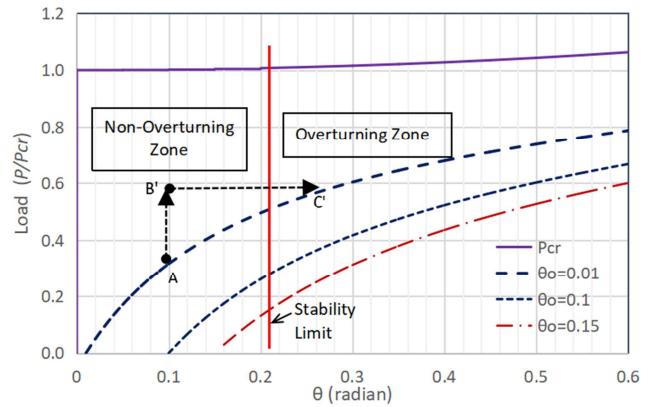

**Figure 9.** Deformation path on soft foundation (e/L=0.185).

4.2. Displacement Path on Ks-θ Curves

Similarly to Figure 9, the overturning mechanism (3) Type of equilibrium transition will be explained again in this section by using the Ks-θ curves [5, 6]. Figure 10 shows the equilibrium curves in Ks-θ plane, which is obtained by Eq. (2), as an example for the machine with the weight P=980kN, the eccentricity e/L=0.185 and the different initial inclinations. The vertical line is the stability limit shown just for reference.

The curve of the initial inclination θ_0 =0.01 in Figure 10b is taken from Figure 10a, from which the required Ks is found 6470kNm/rad. A similar loading path in Figure 9 on P-θ plane is presented in Figure 10b on Ks-θ plane this time. Namely, the machine is located at the present equilibrium position A and happens to move to the point B or B' on the soft foundation (small Ks), at which the equilibrium becomes unbalanced. Then, the machine will move to the position C or C' to keep equilibrium. Since the equilibrium point C is still in non-overturning zone, the machine will not overturn while the machine at the point C' beyond the stability limit will overturn. From this explanation, it is understood that the area surrounded by the stability limit and the required Ks in Figure 10b is the overturning zone derived by the mechanism (3) Type of equilibrium transition.
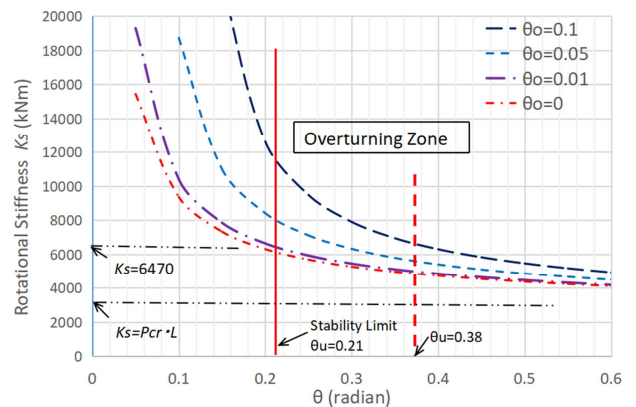
a. Ks-θ curves (P=980kN, e/L=0.185).
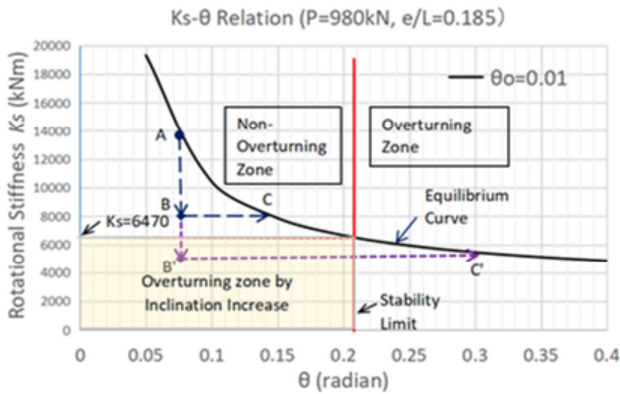
b. Equilibrium transition in Ks-θ curves.

Figure 10. *Equilibrium Curves in Ks-θ Plane.*

Figure 11. *Overturning test.*

5. Preliminary Model Test

A preliminary simple model test was carried out by the author, et al. [12]. Figure 11 shows a scene of the test. The representative results are plotted by the critical load-height relations in Figure 12 in comparison with the theoretical curves. The theoretical curves are calculated by Eq. (3) based on the measured rotational stiffness Ks for the diferent foundations.

It can be said that the test results basically agree with the theory. A interesting point in Figure 12 is that there is a tendency of larger difference between the test and the theory in small load or large height range. This can be explained by considering the effects of initial imperfections shown in Figure 13. The test results in Figure 12 should include the effects due to the unavoidable initial imperfections by which the overturning load is reduced significantly.

Figure 13 shows the load-displacement curves with the initial inclinations; two stablity limits are placed just for explantion purpose. For a certain initial inclination, say θ_0

=0.02 as shown in Figure 13, it is obvious that the critical load P/Pcr is smaller for the smaller stability limit. Note that the theoretical curves in Figure 12 are Pcr calculated by Eq. (3) without the initial inclination. Therefore, it is rational that the test result P/Pcr will be smaller if the initial imperfections exist.
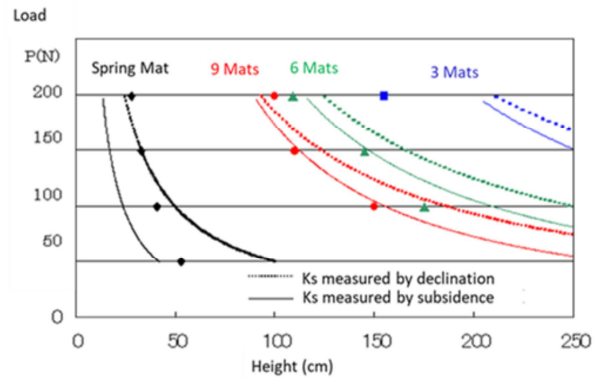

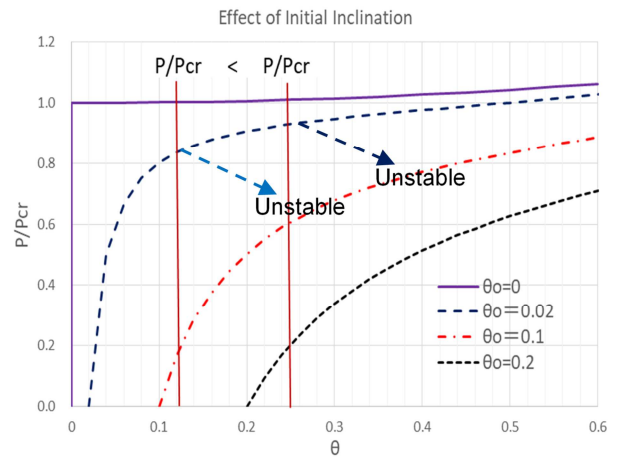***Figure 12.*** *Test results of load-height relations.*

Figure 13. *Effect of initial inclination on overturning.*

6. Computer Structural Analysis by TDAPIII

6.1. Load-Displacement Curves

In this section, the theoretical results are examined by using the computer numerical analysis TDAPIII (Time-domain Dynamic Analysis Program in 3-dimension [13]. Figures 14 through 16 show the load-displacement curves obtained by TDAPIII for three different rotational stiffness Ks=3293, 5000, and 7000kNm/rad with a constant load height L=3.36m [7, 10]. The vertical axis is the number of load increments N up to the critical load Pcr which is calculated from Eq. (3), thus N=1000 means the critical load Pcr, and the transverse axis is the displacement θ. The vertical axis in this case consequently expresses the non-dimensional load P/Pcr, which leads all Figures 14 through 16 to the same results.
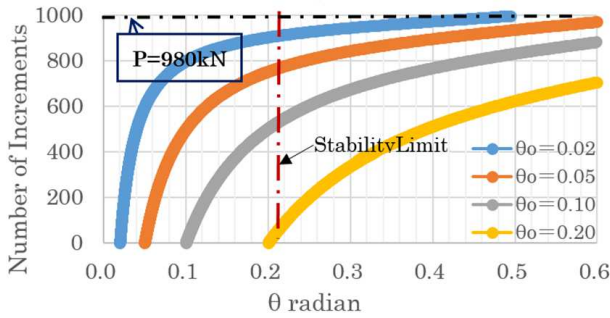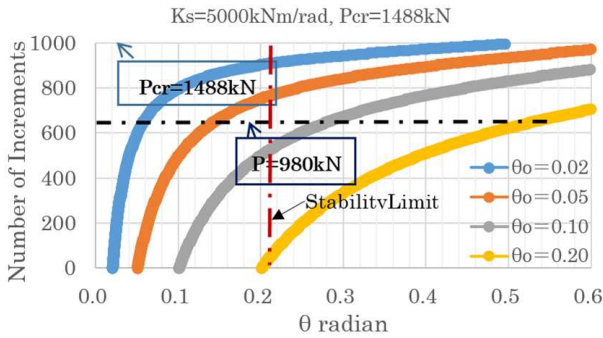
Figure 14. *Load-displacement curves (Ks=3293kNm/rad).*

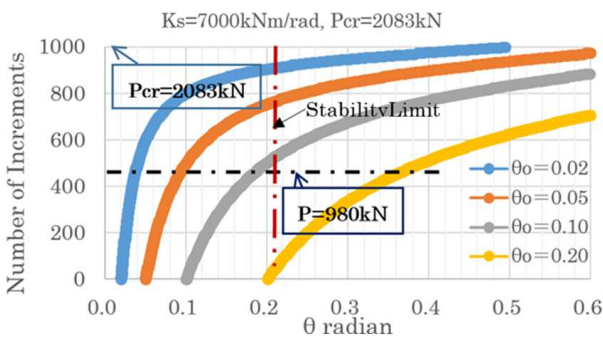
Figure 15. *Load-displacement curves (Ks=5000kNm/rad).*

Figure 16. *Load-displacement curves (Ks=7000kNm/rad).*

The figures also coincide with Figure 6, which means that the theoretical results in Section 3 are verified by the computer analysis. In Figures 14 through 16, the load (machine weight) P=980kN is indicated by the horizontal line for reference, of which intersections with the Load-displacement curves gives the displacements of the machine load *P* for the corresponding initial inclination. There is no intersection in Figure 14 because even with no initial inclination the machine will overturn by the overturning mechanism (2) Type of structural instability.

The stability limit angle is also shown by the vertical line in the figures just for explanation purpose. The intersection of the vertical stability limit line and the horizontal load line indicates the permitted initial inclination θ_0 for the machine on the soft foundation. For instances, in cases of Ks=5000kNm/rad of Figure 15 and 7000kNm/rad of Figure 16 the permitted initial inclinations are about 0.075 and 0.12, respectively. It can be observed that the larger the rotational stiffness *Ks*, in other words the stronger the foundation, the larger the initial inclination θ_0 is permitted.
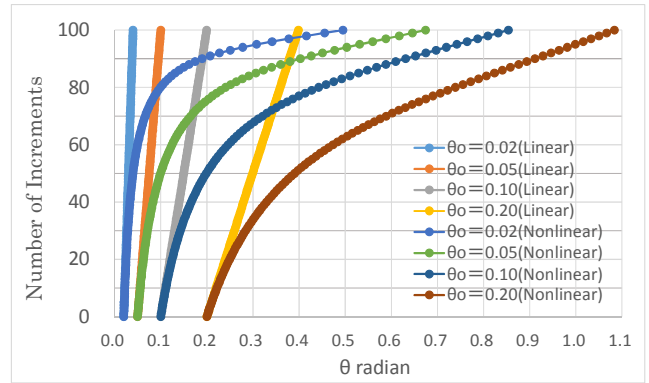

Figure 17. *Comparison between 1st and 2nd analysis (Ks=3293kNm/rad).*

6.2. Comparison Between 1st and 2nd Order Analyses

Any structural stability has to be analyzed by second order. The results in Figures 14 through 16 are analyzed by TDAPIII using the geometric nonlinear elastic beam element. Here, the analyses using the elastic linear and non-linear elements are compared in Figure 17. Difference is obvious: the linear analysis has a straight line and the non-linear analysis involves curvature. Naturally, the non-linearity of the displacement appears remarkably as the load approaches to the critical load.

6.3. Eigenvalue Analysis

The critical overturning load of Eq. (3) can be obtained by the computer numerical analysis. The blue line in Figure 18 is the theoretical load (see the ordinate on left)-displacement path: the displacement is zero until the critical load (fundamental path), and after that the displacement will increase slightly (post-buckling path) [11]. The theoretical post-buckling path can be obtained by taking both the initial inclination and the eccentricity as zero in Eq. (4).

The computer analysis gives the load (see the ordinate on right)-displacement path shown by the brown line [7]. In this analysis the critical load is take as *Pcr*=1200kN, therefore *P*=980kN corresponds to N=980 on the right ordinate which means *P/Pcr*=0.98 on the left ordinate. A good coincidence between the two analyses can be observed except at the corner of the critical load (eigenvalue) in Figure 18. This discrepancy is inevitable in any numerical analysis such as computer analysis. A similar outcome can be seen in the elastic buckling analysis of columns [11].
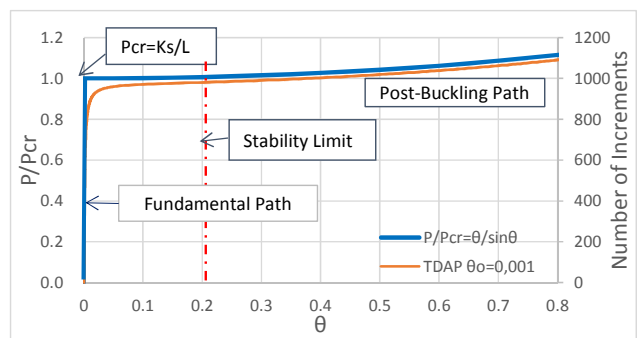

Figure 18. *Eigenvalue analysis (Pcr=980kN).*

7. Foundation Strength Coefficient

In this section, merely the outline of relating the rotational stiffness to the ground strength is presented. By knowing the ground strength coefficient, the computer analysis can be more effectively applied.

As described previously, the required rotational stiffness is obtained from Figure 10b. By the definition in Eq. (1), the rotational stiffness is the righting moment at the displacement θ=1radian. Therefore, at the stability limit θu, the righting moment Mt in Figure 19 is equal to $Ks\theta u$, which works to the foundation. Considering the machine with the crawler arrangement shown in Figure 19, the reaction force R on one crawler generated by the righting moment can be calculated by Eq. (7).

$$R = \frac{Ks\theta u}{d+b} \tag{7}$$

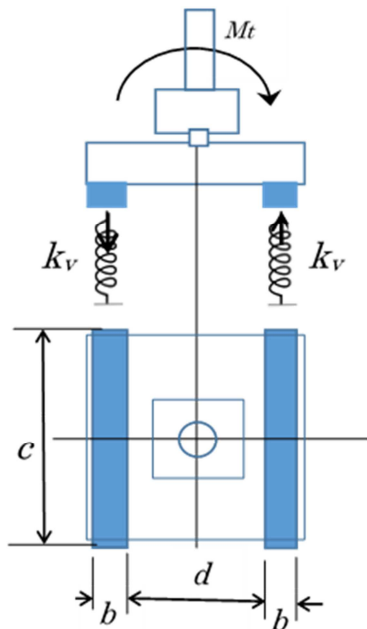in which d=distance between the crawlers, and b=width of crawler.

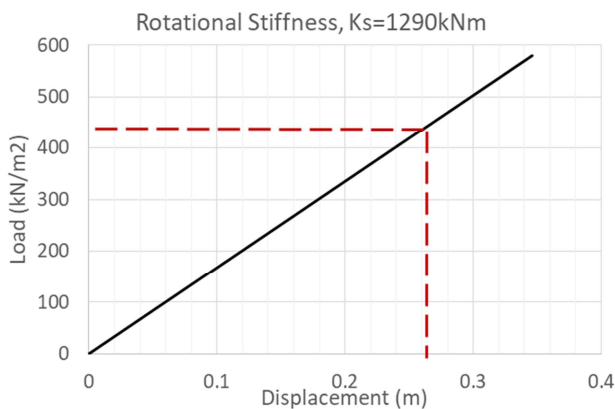**Figure 19.** *Spring stiffness of foundation.*

Figure 20. *Foundation strength coefficient, kv.*

As an example, in the following discussion, let's assume b=0.66m, c=3.4m and d=2.0m in Figure 19. Note that Eq. (7) is based on the first order analysis for simplicity. Sum of the reaction force R and a half of the machine weight $P/2$ is the acting force from the crawler to the foundation. Therefore, the foundation (ground) strength must sustain this total force. If not, the machine will overturn.

Here, let us discuss the required foudation strength in case of Figure 10b, in which the required rotational stiffness is shown as Ks=6470kNm/rad. According to the definition of the rotational stiffness, the actual working overturning moment becomes Mt=6470x(0.21-0.01)=1290kNm, in which the stability limit θu =0.21 and the initial inclination θo =0.01. Therefore, the sum of the reaction R by Eq. (7) and a half of the weight makes 975kN.

On the other hand, at the stability limit the reaction force status is illustrated in Figure 2 (b) neutral. It can be found from the figure that the maximum reaction force on one crawler is equal to the machine weight 980kN which is close to the sum 975kN, and the minimum is zero on the other side of crawler.

The average pressure force on the crawler is 980/(3.4x0.66) =436kN/m². At the stability limit, the subsidence displacement of the crawler in Figure 19 is (2.66/2)sin0.20 =0.26m. The relationship between the pressure force and the subsidence displacement of the foundation is shown in Figure 20, of which the inclination gives the foundation strength coefficient, kv. It can be found that in this case the required vertical foundation strength coefficient is kv=436/0.26 =1680kN/m³. The foundation strength coefficient must be larger than the required value. In actual situation at the construction site, because of the unexpected oscillation while moving or the ground inclination the allowable strength coefficient in the planning has to contain the safety factor.

In this paper, for simplicity the stiffness of the rotational spring is assumed as linear. Development of the relationship between the rotational spring stiffness and the actual ground strength including the nonlinearity is an important theme to investigate the overturning mechanism in the future.

8. Conclusions

The overturning occurs not only by the overturning moment but also by the structural instability. In this paper, the overturning mechanisms which are previously investigated based on the structural stability theory are summarized and verified by using the computer numerical analysis.

The overturning mechanisms are classified into the three: (1) Type of overturning moment, (2) Type of structural instability and (3) Type of equilibrium transition. Among them, (3) Type of equilibrium transition is discussed as the overturning mechanism on the soft foundation in connection with the other mechanisms.

The stability status can also be divided into the three: (a) stable, (b) neutral and (c) unstable, which follows the stability

concept in two ways: displacement-wise and load-wise. Although the overturning eventually occurs when the displacement exceeds the stability limit angle displacement -wise, the load causes the instability which may result in the overturning as well. In this paper, the overturning mechanism on the soft foundation is described with regards to those mechanisms and stability status.

Some other aspects such as the simple model test, the eigenvalue analysis by the computer numerical analysis and the relation between the rotational spring stiffness and the foundation soil strength are also discussed.

In general, the computer analysis is more practical and useful than the theory in investigating the overturning mechanism. It would be possible to include the non-linearity of the ground support or 3-dimensional effect. In the future, in order to avoid the overturning accidents the results presented in this paper are expected to give useful information.

References

[1]   Nikkei Construction, Special Issue. (2000). Accidents under Construction, Preventing Measures for Recurrence by Learning from Great 70 Accidents, Overturning Accidents of Heavy Machines, Nikkei BP, November. (in Japanese).

[2]   Pile Driving Contractors Association (PDCA). (2019). WORKING PLATFORMS, Posted in Pile Driver Magazine. Edition, 3, 2019**. https://www.piledrivers.org/blog/working-platforms.htm.

[3]   Pile Driving Contractors Association (PDCA). (2017). Pile Driving Safety and Environmental Best Management Practices, September 19.

[4]   Pile Driving Contractors Association (PDCA). (2021). Working Platforms Recommended Industry Practices.

[5]   Toma S. and Chen W. F. (2022). Overturning Mechanisms of Jacks, Cranes and Pile Driving Machines, Structural Engineering International (SEI), Taylor & Francis Online, 29 July. DOI: 10.1080/10168664.2022.2074339.

[6]   Toma S. (2022). Analysis of Overturning Mechanisms of Pile Driving Machines on Soft Foundation, Kogaku-Kenkyu, Graduate School of Hokkai-Gakuen University, September (in Japanese).

[7]   Toma S. and Hoshino J. (2023). A Study of Overturning Stability of Pile Driving Machines, etc. by TDAPIII, February (to be published in Japanese).

[8]   Japan National Institute of Occupational Safety and Health (JNIOSH). (2020). Disaster Investigation Report - Scaffolding Collapse Occurred at Construction Site of New Building. https://www.jniosh.johas.go.jp/publication/pdf/saigai_houkoku_2020_05.pdf (in Japanese).

[9]   Tome, S. (2021). Causes of Bridge Girder Fall Accidents due to Overturning Jacks, Journal for Japan Society of Safety Engineering, October 60 (5) (in Japanese).

[10] Hori T., Tamate S. and Suemasa N. (2010). Measurement of Shakes and Ground Contact Pressure of a Drill Rig by the Self-Propelled Experiments, Journal of Japan Association of Civil Engineering C. May (in Japanese).

[11] Chen, W. F. and Lui, E. M. (1987). Structural Stability, Theory and Implementation, Chapter 1 General Principles, Elsevier.

[12] Toma, S. (2001). A Study on the Causes of Overturning Accidents of Movable Cranes and Others, 58th Research Report of Hokkaido Branch of Japan Society of Civil Engineers, (in Japanese).

[13] General Purpose 3-Dimensional Dynamic Analysis Program for Civil Engineering and Architectural Use, ARK Information Systems, INC., Tokyo, Japan, https://www.ark-info-sys.co.jp/ jp/product/tdap/English/.